# IMMUNOHISTOCHEMICAL CRITERIA OF PULMONARY ARTERY CIRCULAR DENERVATION EFFICIENCY IN EXPERIMENT (animals, pigs)

**Trofimov N.A.[1], Nikolskiy A.V.[2], Rodionov A.L.[3], Egorov D.V.[4], Surkova T.V.[5]**

[1,2,3,4,5]Chuvash State University, 15 Moskovskiy Ave., 428015 Cheboksary, Russian Federation

Email: nikolai.trofimov@mail.ru

## Abstract

Research objective. Evaluation of the influence of various modes of radiofrequency circular exposure on immunohistochemical parameters of pulmonary trunk tissues in the experiment on animals (pigs).

Materials and methods. The experiments were made on outbred pigs – 12 animals. During the experiment 3 groups were formed, 4 animals in each. The first experimental group comprised 188 histological samples of pulmonary artery (PA) after circular radiofrequency exposure on PA using an ablator clamp. Two lines of ablation impact on the pulmonary trunk and two lines of impact on each mouth of PA were performed with the formation of 6 ablation lines. The ablation was performed until the target level of tissue impedance between the ablator jaws corresponding to the values for transmural damage was reached. The second experimental group comprised 162 histological samples of PA after circular denervation of the pulmonary trunk and mouths of both PAs according to the described method. The ablation was completed upon reaching 50% of the impedance level relative to the impedance values for transmural damage. The third group – control, without circular radiofrequency exposure (55 histological samples). The obtained material was studied by light microscopy, typical general pathological processes were recorded with the help of staining with hematoxylin and eosin. The changes in the connective tissue (fibrous, muscle) were found with the help of Van Gieson staining. The thermoablative effect degree was assessed using semi-quantitative analysis of pathological processes (Olpred stain intensity assessment). In order to assess the degree of impact on the nerve fibers of different layers of PA, an immunohistochemical study (IHC) of the samples was carried out in all three groups. The expression of S-100 protein and synaptophysin was evaluated.

Conclusion. Average optic density of the samples of the ablation groups was significantly lower than in the control group ($p < 0.001$). When calculating the specific area of the connective tissue disconnection, its greater value was determined in “the edge zones” of the sections in both experimental groups, which is due to mechanical compression of tissues, compaction of their structure and, as a result, an increase in capacitive characteristics as a current collector and conductor for radio frequency rate ( $p = 0.056$). IHC analysis of preparations made it possible to qualitatively assess the damage to the trunks and endings of peripheral nerve fibers in the adventitial and intimal layers of PA section after radiofrequency exposure in the experimental groups.

In the first experimental group the active expression of synaptophysin and protein S-100 of sympathetic nerve fibers was absent in the adventitial and, as a rule, in the intimal layers. In the preparations obtained from PA of animals of the second experimental group, the activity of synaptophysin in synaptic fibers and expression of protein S-100 of endothelium vasa vasorum were also not determined in the adventitial layer. At the same time, the positive reaction of protein S-100 and synaptophysin was observed in the nerve endings and ganglia in the intimal layer of PA preparations of the second group.

The circular denervation of PA using subthreshold rate of radiofrequency exposure corresponding to 50% of the impedance of PA tissues from the corresponding impedance values in case of transmural damage, made it possible to avoid irreversible damage to the nerve endings and ganglia of PA intimal layer, thereby preserving the physiological neuroreflex regulation of PA and entire pulmonary circulation. Thus, the cascade of pathological reflexes, factors of pulmonary hypertension advance connected with the spasm of precapillary mouth of the pulmonary arterioles is turned off.

**Keywords:** secondary pulmonary hypertension, radiofrequency ablation, denervation of pulmonary arteries, histological study.

## INTRODUCTION

The mortality from cardiovascular diseases (CVD) all over the world takes first positions in statistic reports. According to the data of World Health Organization (WHO), 17.5 million people died from CVD in 2019, which is 31% of deaths in the world [1]. Pulmonary hypertension (PH) is one of the urgent issues of cardiovascular surgery [2, 3].

PH is a hemodynamic and pathophysiological state characterized by the increased mean pressure in the pulmonary artery (PPA) ≥ 25 mm Hg at rest measured at through-venous heart catheterization [4]. PH epidemiology affects about 1% of the population, at the age over 65 years it is found with 10% of patients [3]. Nevertheless, the incidence and prevalence rates of various PH clinical groups differ significantly [5, 6].

The PH initial form is mediated by the mutation in 2q33 chromosome responsible for the proliferation of endothelial cells. Secondary PH is a multifactor disease with patients with systemic affection of heart left chambers after past thromboembolisms, chronic diseases of respiratory system on the background of metabolic disorders [4, 7, 8].


| Access this article online | |
|---|---|
| Quick Response Code: | Website: www.pnrjournal.com |
| | DOI: 10.47750/pnr.2022.13.03.122 |


The classification (2018) describes 5 cases of PH: pulmonary arterial hypertension (PAH); pulmonary hypertension connected with the pathology of heart left chambers; pulmonary hypertension associated with respiratory system diseases and/or hypoxemia; chronic thromboembolic pulmonary hypertension and other types of obstruction of pulmonary arteries; pulmonary hypertension with unclear or multiple mechanisms [3, 9, 10].

The increased activity of sympathetic nerve system is one of the universal mechanisms participating in the pulmonary hypertension pathogenesis [11, 12]. According to the experimental data, when the arterial pressure in PA increases and its opening closes completely, the resistance and pulmonary pressure spike [13, 14, 15]. At the same time, the diastolic pressure in left and right ventricles, pressure in aorta and cardiac output remain unchanged. The regularity revealed allows assuming that baroreceptors, providing the reflex arc of pulmopulmonary reflex, are situated close to pulmonary trunk bifurcation [5].

**Address for correspondence: Trofimov Nikolai Aleksandrovich**
Chuvash State University, 15 Moskovskiy Ave., 428015 Cheboksary, Russian Federation
Email: nikolai.trofimov@mail.ru



How to cite this article: Trofimov N.A., Nikolskiy A.V., Rodionov A.L., Egorov D.V., Surkova T.V., IMMUNOHISTOCHEMICAL CRITERIA OF PULMONARY ARTERY CIRCULAR DENERVATION EFFICIENCY IN EXPERIMENT (animals, pigs), J PHARM NEGATIVE RESULTS 2022;13: 811-822.

The histological substantiation of the existence of sympathetic nerve structures in the adventitial layer of pulmonary arteries regulating the tonus of pulmonary arterioles and contributing to increased pressure in pulmonary circulation, was for the first time highlighted by the group of authors supervised by J. Osorio in 1962 [16]. Later, those results were confirmed in the works by B.G. Baylen [17] and C.E. Juratsch [13, 18, 19]. According to the researchers, 80% of sympathetic nerves are situated in proximal and distal sections of pulmonary trunk bifurcation (bifurcation region, mouths of right and left PAs and pulmonary trunk region <2 mm before bifurcation) within 2.5-3 mm from the opening. With pigs, the nerve trunks with large diameters over 300 mcm are concentrated in proximal segments of pulmonary arterial tree, and distal segments are mainly represented by nerve trunks with smaller diameters located close to the opening (< 1 mm) [13]. The arterial baroreceptors are situated in the adventitial layer of the vessel wall, therefore, it is important to selectively act upon the adventitial and partially medial shells to achieve the complete stop of these receptors' functioning.

In 2013 Chen et al. for the first time applied radiofrequency ablation of PA in the area of pulmonary trunk bifurcation in the experiment on animals (dogs). The immediate results of the surgical treatment were encouraging and contributed to significant decrease in pulmonary hypertension [20].

Denervation of pulmonary arteries is a new pathogenetically substantiated treatment method. The denervation procedure can be performed by the method of radiofrequency ablation of the pulmonary trunk, in the vessel wall of which the most part of nerve fibers of the sympathetic nerve system is concentrated [21].

Thus, the new stage of denervation of pulmonary arteries assumes the development of selective and minimally invasive methods of destruction of sympathetic nerve plexuses in PA adventitia without injuring the neighboring anatomic structures.

Research objective. Evaluation of the influence of various modes of radiofrequency circular exposure on

immunohistochemical parameters of pulmonary trunk tissues in the experiment on animals (pigs).

## Materials and methods

The experiments were made on outbred pigs. The work with laboratory animals was carried out according to the investigation protocol in compliance with Geneva Convention of 1985 and Helsinki Declaration of 2000 on humanistic attitude to animals.

The investigation comprised the analysis of the material collected from 12 animals. During the experiment 3 groups were formed, 4 animals in each.

In the first group (experimental) the pigs underwent left-side thoracotomy in the phlebonarcosis state, the pulmonary trunk was identified. The circular mechanical clamping of the pulmonary trunk with an ablator clamp and radiofrequency exposure on the vessel walls with embedded jaw electrodes were carried out. Two lines of ablation impact on the pulmonary trunk and two lines of impact on each mouth of PA were performed with the formation of 6 ablation lines (Figs. 1, 2).

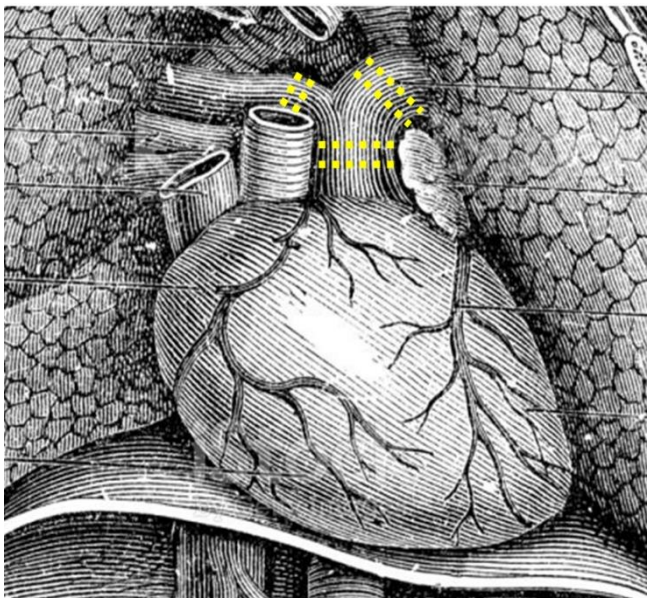

**Figure 1.** Scheme of circular PA denervation

1 – pulmonary trunk, 2 – mouths of right and left PAs, 3 – lines of applying circular ablation action

The radiofrequency exposure was applied in the controlled manner due to the energy supplied from the computer-programmed hardware-based generator (Fig. 2). During the ablation, the continuous hardware-based monitoring of the tissue conductivity with computerized calculation of the impedance and its demonstration in the dynamic graphical form was carried out, as well as by the computational boundaries of the assumed level of transmural damage of the tissues.

**Figure 2.** Circulation ablation of pulmonary artery with an ablator clamp in the experiment

The ablation was performed until the target impedance level of the tissues between the ablator jaws corresponding to the values for the transmural damage was reached. After PA circular denervation was completed, all animal groups were taken away from the experiment. The pulmonary trunk in the region of its bifurcation into right and left branches was studied (Fig. 1).

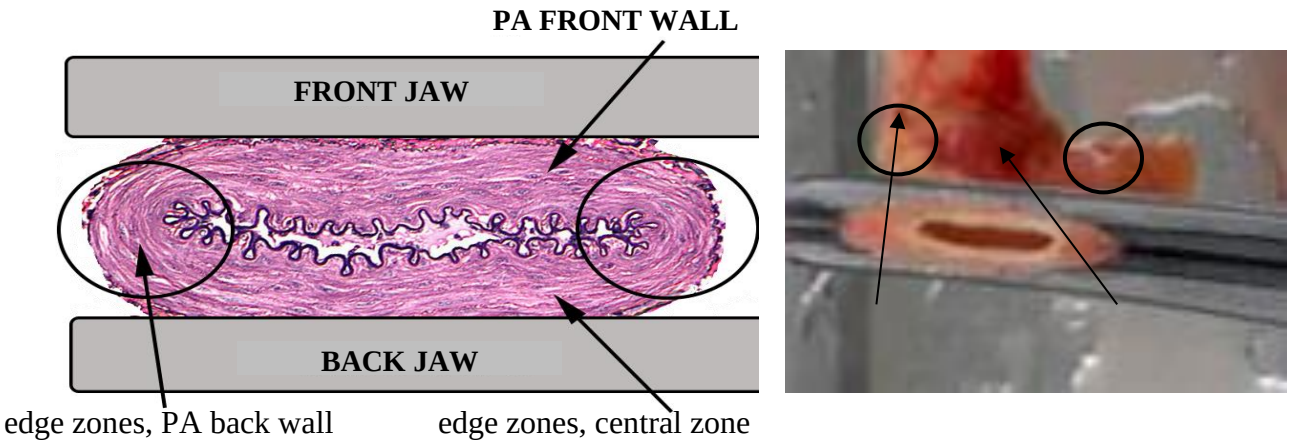


**Figure 3.** Photo of PA fixation in jaws under their cross-clamping

The first group was represented by 188 histological samples and split into subgroups A and B. During the circular ablation impact on the pulmonary artery tissues, the parallel jaws of the ablator clamp non-uniformly act upon the pulmonary trunk forming conditional "edge zones" in the vessel duplication areas (Figure 3). Therefore, it was considered reasonable to distinguish two subgroups in the first experimental group: 1A and 1B based on the impact area. Subgroup 1A comprised the regions of the central zone of PA cross cut (92 histological samples). Subgroup 1B comprised the regions of "the edge zone" (96 histological samples).

The second experimental group comprised 4 animals who underwent left-side thoracotomy in the phlebonarcosis state with PA identification and circular denervation of the pulmonary trunk and mouths of both PAs with the formation of six impact lines following the described technique. The ablation impact mode in the second experimental group was controlled by the impedance level of PA tissues. The ablation was completed upon reaching 50% of the impedance level relative to the impedance values for transmural damage. The material was collected in 2 hours after the completion of PA circular denervation, then all animal groups were taken away from the experiment. The pulmonary trunk was collected in the region of its bifurcation into right and left branches (162 histological samples).

The second group consisted of subgroup 2A – regions of PA cross cut central zone (76 histological samples) and subgroup 2B comprising the regions of "the edge zone" of the cuts of preparations (86 histological samples).

The third group (control group) consisted of 4 animals who underwent phlebonarcosis with further left-side thoracotomic access and collection of PA samples without circular radiofrequency exposure. Then the animals were taken away from the experiment (55 histological samples).

After that two cuts were formed from PA wall samples obtained, in each of which 6 fields were singled out for visual analysis, and then, in the course of finding the optic density, up to ten additional repeated computations were made for each vision field. After the radiofrequency impact onto PA material, all samples were exposed in 10% solution of neutral buffered formalin. All exposed material was in the solution with the volume 10 and more times exceeding the volume of the material itself. The samples were treated in the solution within 36 hours at room temperature.

The material obtained was studied by light microscopy method, typical general pathological processes were recorded with the help of staining with hematoxylin and eosin. The changes in the connective tissue (fibrous, muscle) were found with the help of Van Gieson staining. The thermoablative effect degree was assessed using semi-quantitative analysis of pathological processes (Olpred stain intensity assessment), computed for all ten vision fields of all pathological processes revealed. The possibility of their mathematical assessment was carried out due to the application of computer morphometry demonstrated on the photos of the preparations' cuts obtained by photo camera OlympusSP350 in the optics of microscope LeicaCME.

In order to assess the degree of impact on the nerve fibers of different PA layers and vasa vasorum in PA adventitia, an immunohistochemical study (IHC) of the samples was carried out in all three groups. The expression of S-100 protein in sympathetic nerve fibers and endothelium vasa vasorum was evaluated where it is obligately present and expressed under normal flow of metabolic processes and preserved transport function of cell membranes. The expression of synaptophysin – glycoprotein of synaptic membranes in sympathetic nerve fibers was studied in the preparations under investigation, the absence of expression of which indicates the irreversible affection of the conductive nerve tissue.

The results were statistically assessed with the application of software "SPSS Statistics 26". The numerical data were described using mean and standard deviation (M±σ). To check the statistical hypotheses, Student t-test was applied if

the normal distribution of initial data was available, and in case of unequal dispersions Mann-Whitney rank-sum test was used. When building up the contingency tables to compare and check the samplings of all 4 groups, Kruskal-Wallis test (for numerical and rank-sum data) and Pearson's chi-squared test (for qualitative data) were applied. The differences were considered significant at the level $p<0.05$ [29].

The first stage of the investigation of the obtained histological material of PA tissues was light microscopy (LM) to reveal the qualitative indications of radiofrequency and mechanical impact.

The clear differentiation of PA wall layers with the preserved architectonics was visualized in the control group preparations under LM, the phenomena of pericellular and pericapillar swellings were absent, the areas of fibrinoid necrosis were not determined (Fig. 4).

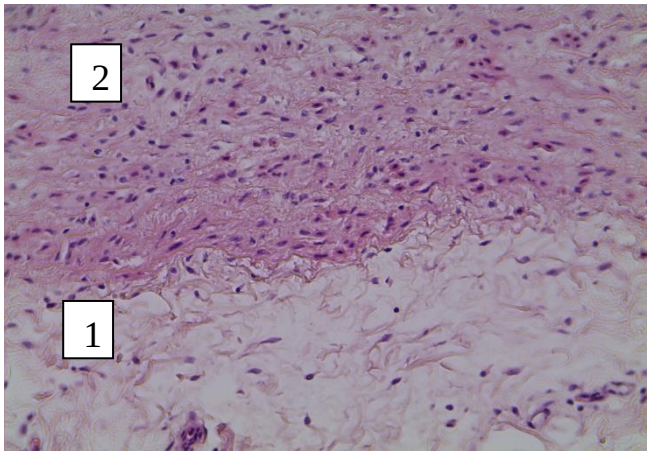


**Figure 4.** LM. Central region (control group) of PA wall cross cut (magnification: 200x, staining: hematoxylin and eosin)

Designations: 1 – adventitial layer with preserved architectonics, pericellular swelling is absent; 2 – structure of medial layer cells is preserved, pericellular swelling is absent

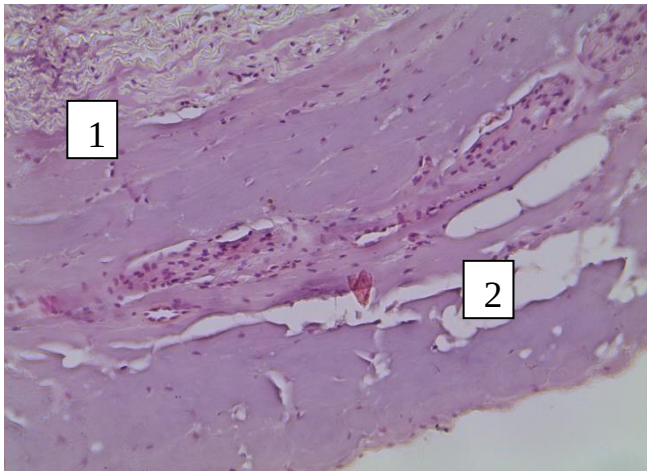


**Figure 5.** LM. Central region (group 1A) of PA wall cross cut in the area of radiofrequency exposure (magnification: 200x, staining: hematoxylin and eosin)

Designations: 1 – fibrinoid necrosis in adventitial layer, 2 – formation of cavity structures in adventitial layer

The regions of fibrinoid necrosis, phenomena of disorganization of elastic muscle fibers with the phenomena of karyorhexis and karyolisis in firoblasts and smooth muscle myocytes were observed in the first experimental group in central areas (subgroup 1A). The changes described above in the consistent manner were registered in the adventitial shell with the distribution onto PA wall medial area, sometimes the damage had transmural character with the affection of subendothelial structures and was represented in the samples in the form of fibrinoid necrosis and metachromasy of the connective tissues fibers (Fig. 5).

The depth and area of fibrinoid necrosis, as well as metachromasy phenomena were more vividly expressed and more often had the transmural character in "the edge zones" (subgroup 1B); after the radiofrequency exposure the deep transmural disorganization of the walls of PA tissue was observed in the area of mechanical compression of the duplication of PA tissues (Fig. 6).

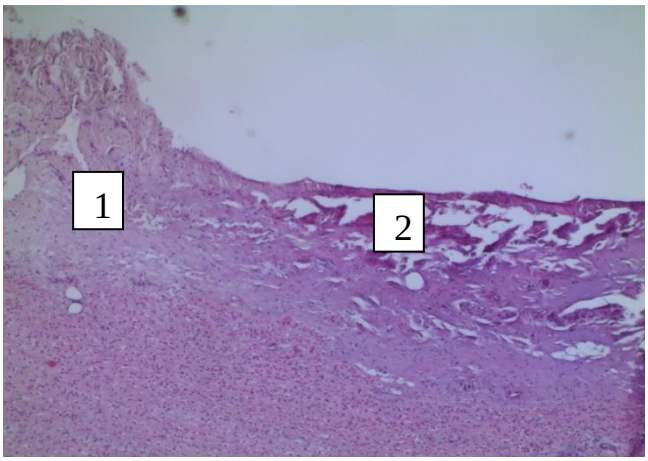


**Figure 6.** LM. "Edge zone" (group 1B) of the cross cut of ablation impact region (magnification: 200x, staining: hematoxylin and eosin)

Designations: 1 – fibrinoid necrosis in adventitial layer, 2 – formation of cavity structures in adventitial layer

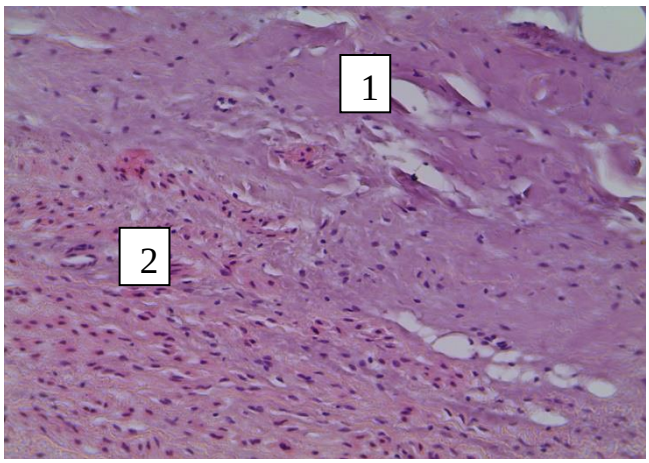


**Figure 7.** LM. Central region (group 2A) of the cross cut of ablation impact region (magnification: 200x, staining: hematoxylin and eosin)

Designations: 1 – separation of fibers of adventitia structures, emergence of cavity formations of different sizes, 2 – myxomatosis, moderate pericellular and pericapillar swelling of medial layer structures

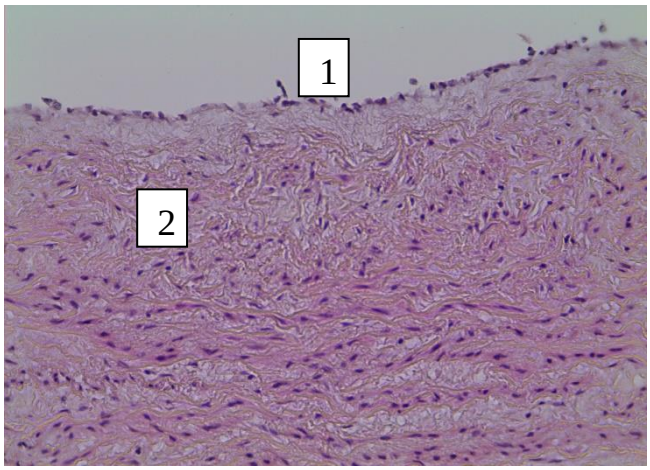


**Figure 8.** LM. Central region (group 2A) of ablation impact cross cut (magnification: 200x, staining: hematoxylin and eosin)

Designations: 1 – endothelium without damages, 2 – intimal layer without damages

The changes in PA tissues of the second experimental group after the radiofrequency exposure were registered under light microscopy in the adventitial layer in the form of fibrinoid necrosis with the transition onto the medial layer in the form of myxomatosis, pericellular and pericapillar swelling phenomena (Fig. 7). In the second investigation group the endothelium and intimal structures did not demonstrate the indications of irreversible structural damages in the preparations of pulmonary artery under light microscopy (Fig. 8).

Van Gieson staining of the preparations was also used to assess the depth (transmurality) of thermoablation effect onto the connective tissue. Pathological indications were absent on PA cross cuts in the control group: separation of collagen fibers and swelling of elastic fibers, fibrinoid necrosis zones were absent (Fig. 9).

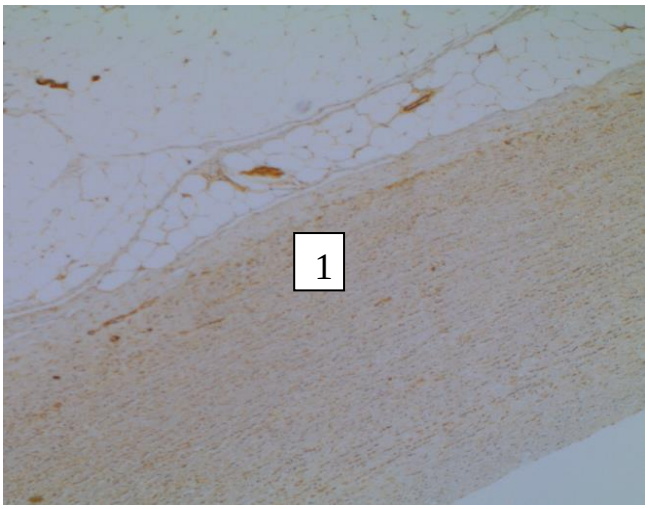


**Figure 9.** LM. (Control group). Cross cut region of ablation impact (magnification: 200x, staining: hematoxylin and eosin)

Designations: 1 – separation of collagen and swelling of elastic fibers are absent in medial layer and adventitia, fibrinoid necrosis zones are absent

On the cuts of tissues stained according to Van Gieson, the regions of disorganization of the connective tissue fibers were determined in the preparations of subgroup 1A with the distribution onto PA adventitial and medial layers in the central zone. In the tissues of "the edge parts" of the vessel (subgroup 1B) the regions of fiber separation, disorganization of subendocrinal areas were registered apart from the abovementioned changes (Fig. 10). The transmural character of the damages of PA walls was determined in all preparations of subgroup 1B.

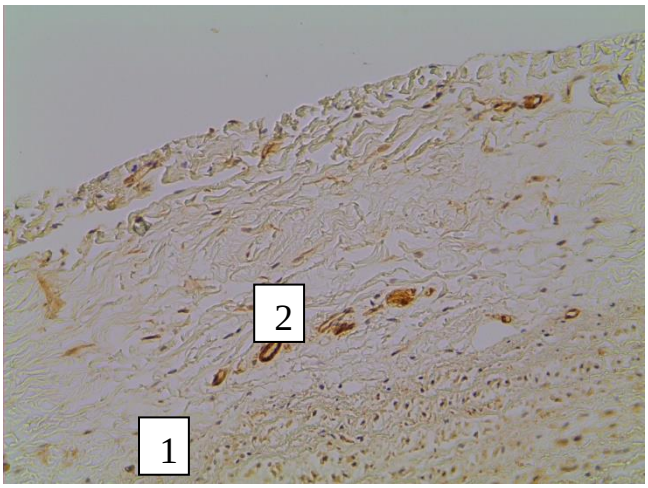


**Figure 10.** LM. "Edge zone" (group 1B) of ablation impact region cross cut (magnification: 200x, staining: hematoxylin

and eosin)

Designations: 1 – regions of destruction of fibrous tissue fibers in adventitial layer, 2 – perivascular swelling of vasa vasorum

The immunohistochemical investigation (IHC) was carried out for the selective assessment of the damages of nerve fibers of intimal and adventitial layers of PA walls, as well as for the assessment of the structures of PA vasa vasorum.

When conducting IHC, a high expression of protein S-100 in sympathetic nerve fibers located intimally and in the adventitial layer as well as in the endothelium of PA vasa vasorum was revealed in PA wall in the control group (Fig. 11), synaptophysin expression was also high in the control group (Fig. 12).

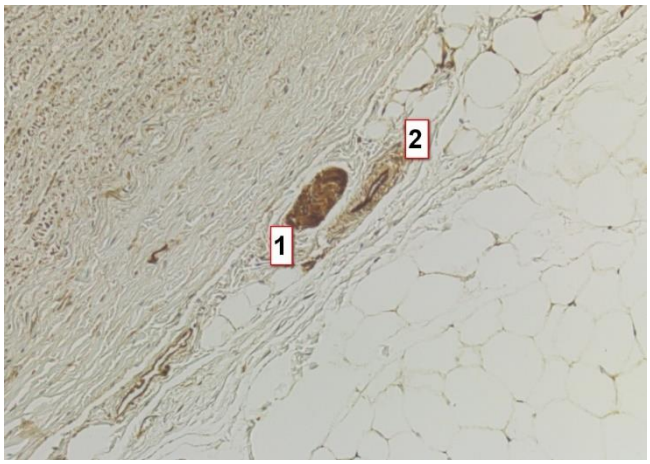


**Figure 11.** LM (IHC). Control group. Expression of protein S-100 in pulmonary artery wall. Magnification: 200x

Designations: 1 – sympathetic nerve fiber providing intensive positive staining for protein S-100, 2 – vasa vasorum endothelium providing intensive positive coloring for protein S-100

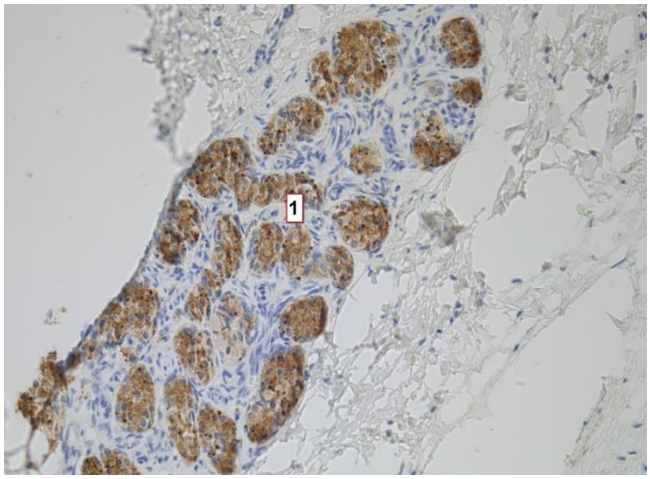


**Figure 12.** LM (IHC). Control group. Expression of synaptophysin in sympathetic nerve fibers. Magnification: 200x

Designations: 1 – sympathetic nerve fibers providing intensive positive staining for synaptophysin of synaptic membranes

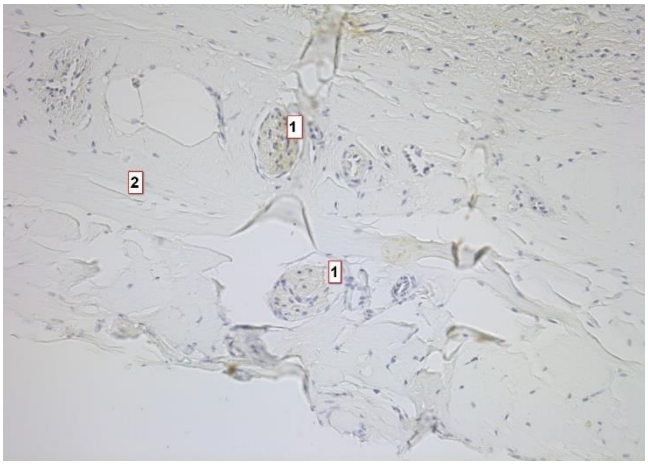


**Figure 13.** LM (IHC). Group 1A. Absence of expression of protein S-100 in sympathetic nerve fibers in the zone of irreversible ablation damage of PA adventitia. Magnification: 200x

Designations: 1 – sympathetic nerve fibers, without expression of protein S-100,

2 – zone of ablation damage of pulmonary artery adventitial shell

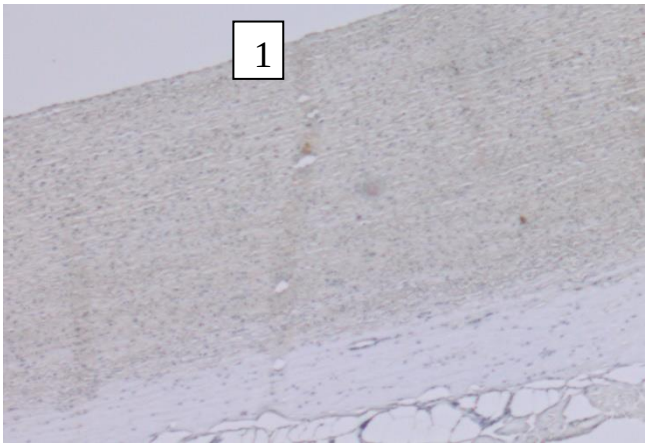


**Figure 14.** LM (IHC). Group 1B. Absence of expression of protein S-100 in sympathetic nerve fibers in the zone of intima irreversible damage. Magnification: 100x 100

Designations: 1 – sympathetic nerve fibers, without expression of protein S-100

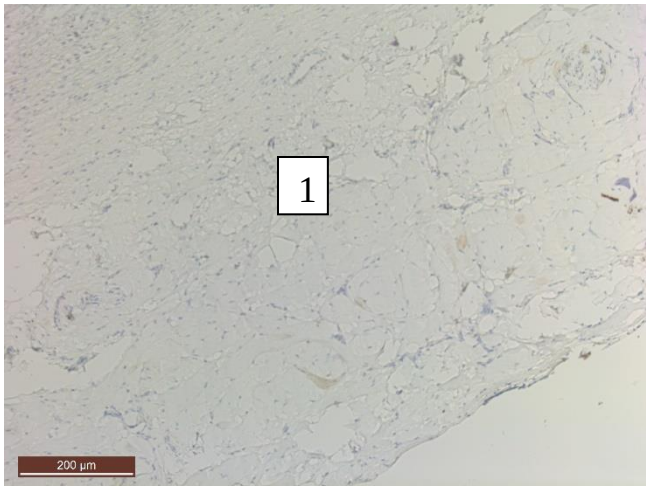


**Figure 15.** LM (IHC). Group 1B. Negative reaction to protein of synaptic membranes in sympathetic nerve fibers in the zone of adventitia irreversible damage. Magnification: 100x

Designations: 1 – absence of reaction to synaptophysin in sympathetic nerve fibers

When conducting IHC, the absence of expression of protein S-100 in sympathetic nerve fibers located both intimally and in adventitia were determined in subgroups 1A and 1B of the first experimental group (Figs. 13, 14), the negative reaction to the protein of synaptic membranes in sympathetic nerve fibers in the abovementioned zones was also revealed (Fig. 15).

During IHC analysis, the positive expression of protein S-100 and synaptophysin in the nerve fibers of intimal layers of subgroups 2A and 2B was noted in the second experimental group (Fig. 16). The reaction to the protein of synaptic membranes, as well as vasa vasorum endothelium to protein S-100 in PA adventitial layer was negative (Fig. 17).

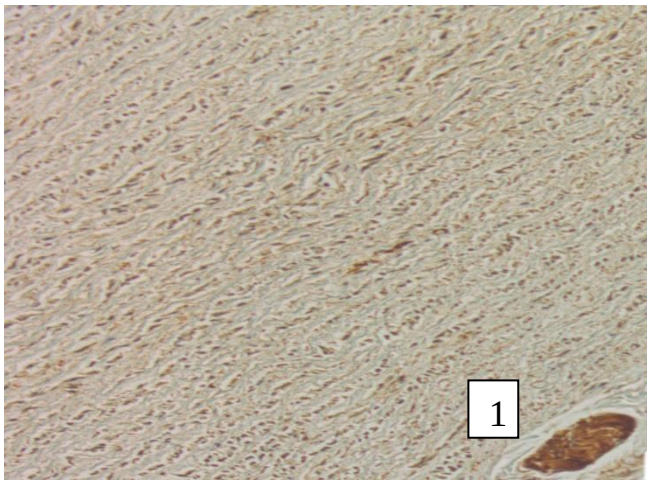


**Figure 16.** LM (IHC). Group 2B. Expression of protein S-100 in intimal layer of pulmonary artery wall. Magnification: 200x

Designations: 1 – sympathetic nerve fiber providing intensive positive staining for protein S-100

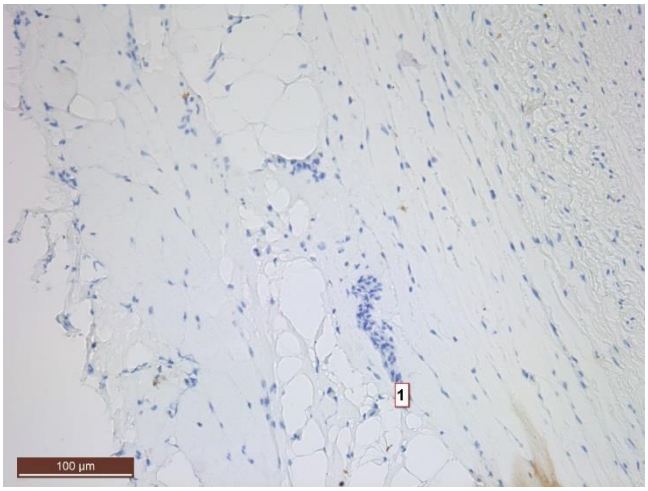


**Figure 17.** LM (IHC). Group 2A. Negative reaction to protein of synaptic membranes in sympathetic nerve fiber of adventitial layer. Magnification: 200x

Designations: 1 – absence of reaction to synaptophysin in sympathetic fiber

The results of light microscopy and IHC objectively demonstrated the depth and degree of changes in PA preparations of experimental groups in the investigation after PADN procedure.

## Results and discussion

The effect of radiofrequency exposure and mechanical impact by the ablator clamp jaws on the pulmonary artery tissues was evaluated based on the score method of semi-quantitative analysis of pathological processes (assessment of staining intensity by Olpred) (Fig. 18).

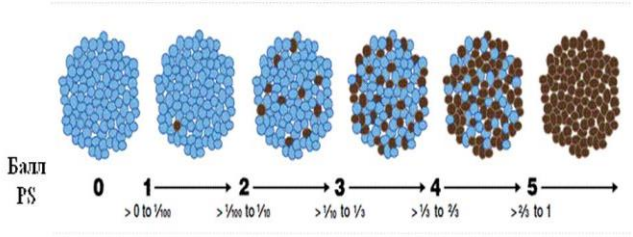


**Figure 18.** System of score assessment of staining intensity by Olpred

The table on each indication for all investigation groups was formed to conduct the intergroup analysis of histological results (Table 1).

The analysis of morphometrical and morphological data obtained during the experiment: area and depth of fibrinoid necrosis, availability of metachromasy, phenomena of disintegration of collagen fibers evidently demonstrated

deeper changes in PA wall after the circular denervation in the first experimental group in relation to the second experimental group.

The damage of nerve fibers in the first group, practically obligately had transmural character and was confirmed by ICH, in particular, by the absence of synaptophysin expression and negative reaction to protein S-100 of sympathetic nerve fibers both in adventitial and intimal layers of PA.

**Table 1.** Analysis of pathological indications of radiofrequency exposure and mechanical impact

| Pathological indication | 1st experimental group | | 2nd experimental group | | Control group (n=55) |
|---|---|---|---|---|---|
| | 1A (central part, n=92) | 1B (edge part, n=96) | 2A (central part, n=76) | 2B (edge part, n=86) | |
| Fibrinoid necrosis | 3 | 3-4 | 2 | 2-3 | 0 |
| Depth of fibrinoid necrosis in the vessel wall (mcm) | 587 ± 84 | 726 ± 58 | 286±54 | 322±74 | 0 |
| Area of fibrinoid necrosis to the total area of the vessel wall (in %) | 14.7 ± 5.0 | 23.4±8.1 | 8.1 ± 3.3 | 12.1± 4.2 | 0 |
| Metachromasy | 2-3 | 4 | 2 | 2-3 | 0 |
| Disintegration of media collagen fibers | 3 | 4 | 2 | 3 | 0 |

It should be pointed out that the most density of pathological indications was observed in the preparations of "the edge zones" (subgroups 1B and 2B) of each separately taken experimental group, which is probably conditioned by the mechanical compression of the tissues, compaction of their structure and, consequently, the improvement of capacity characteristics as a current collector and conductor for radiofrequency energy. The indications of considerable pathological disorganization of PA tissues were not observed in the control group, and indexes of ICH investigation demonstrated positive synaptophysin expression and positive reaction to protein S-100 of sympathetic nerve fibers both in adventitial and intimal layers of PA.

To compare the disorganization degree of fibrous structures of the vessel media the optic density index was calculated, which equals the decimal logarithm of the difference of light transmission through the object (Table 2). The mean optic density of the samples of the first ablation group was evidently lower than of the second and control groups ($p<0.001$) despite the presence of differences in the disorganization degree of fibrous structures of the connective tissue of the middle PA layer between the samples of the subgroups (subgroup 1A – 0.1665±0.0025, subgroup 1B – 0.1505±0.0022). When calculating the specific area of connective tissue disintegration, its average value in the samples of the central part (subgroup 1A) was 30%, and in the samples of "the edge part" (subgroup 1B) – 43.2% from the area of the tissues in the visual field. The similar correlation of the values of comparative optic density of PA wall and mean specific area of disorganization of the connective tissue was observed in the preparations of the second group, respectively subgroups 2A and 2B (subgroup 2A – 0.2177±0.09, subgroup 2B – 0.1948±0.042).

**Table 2.** Comparative assessment of density and distribution degree of determined pathological indications

| Pathological indication | 1st experimental group | | 2nd experimental group | | Control group (n=55) |
|---|---|---|---|---|---|
| | 1A (n=92) | 1B (n=96) | 2A (n=76) | 2B (n=86) | |
| Mean comparative optic density of PA wall (M±σ) | 0.1665* ±0.025 | 0.1505* ±0.0022 | 0.2177* ±0.09 | 0.1948* ±0.042 | 0.3326* ±0.05 |
| Mean value of specific area of disorganization of connective tissue ($p\pm\sigma_p$%) | 30±4.2 | 43.2±1.9 | 21.4±1.6 | 28.9±2.2 | - |

The value of comparative optic density of PA wall was also greater in "the edge zones" of subgroup 2B B – 28.9% in relation to the value in subgroup 2A – 21.4%, respectively. The described differences in morphometrical indexes of "the edge zones" from the central regions in the experimental groups can be explained by the factor of mechanical impact of ablator clamp onto the medial layer of the artery wall at bending. However, the tissue compaction has probably the primary meaning, and, as a result, the improvement of its current conductive and capacity characteristics resulting in increased total effective dose of the delivered radiofrequency energy, and, consequently, in increased pathological changes in PA wall.

The evident morphological criteria of irreversible destruction of sympathetic nerve fibers and ganglia circularly in the adventitial layer of the pulmonary trunk and bifurcation of PA applying both investigated ablation modes were obtained during the experiment. However, the application of the first ablation mode in the first experimental group was accompanied by the obligate affect of nerve structures of the intimal layer in "the edge zones" (subgroup 1B), as well as in some regions of the central impact zone (subgroup 1A).

Thus, the reflexogenic zones and baroreceptors located in the intimal layer of the pulmonary artery main branches were damaged in the first experimental group, which could result in Parin's reflex turn-off. The reflexive mechanism of venous return to the heart and pulmonary vessels is very important and is connected with the impact of elevated intravascular pressure in PA on the intima baroreceptors of PA, as a result, the frequency of heart beat and intravascular pressure in systemic circulation decrease, which, eventually, decreases the venous return to the pulmonary circulation vessels. Parin's reflex plays an important role in the off-loading of pulmonary circulation vessels protecting the right ventricle from the overload and preventing decompensation of pulmonary circulation, including the development of acute pulmonary edema. Therefore, the damaging of the intimal layer of the artery vessels will have a negative effect onto the work of one of the compensatory mechanisms activated with patients in the course of LH development.

The results of the application of the second mode of PA radiofrequncy ablation in the second experimental group allow making the conclusion on the lack of systemic damages of vasoconstrictive sympathetic nerve fibers in the intimal layer of PA wall samples under investigation. Thus, the execution of circular denervation of pulmonary trunk and mouths of PA in the mode of radiofrequency exposure sufficient to achieve only 50% level of tissue impedance in relation to the impedance values during transmural damage, allowed producing the circular damage of PA adventitia not destructing the reflective zones in the artery intimal layer.

## Conclusion

The morphometrical, morphological and immunochistochemical criteria of the efficiency of two different modes of circular radiofrequency denervation of pulmonary artery were analyzed in the experiment. The results of three groups were analyzed: first experimental group – animals whose PA was taken after the circular denervation following the described technique with the impedance indexes corresponding to transmural damage at the moment of ablation. The second experimental group comprised pigs whose PA was taken after the circular denervation following the described technique but with the application of less radiofrequency exposure rates sufficient to achieve only 50% level of the tissue impedance in relation to the impedance values under transmural damage. The third control group did not undergo ablation.

At the first stage, the morphological pathological indications in different PA wall layers were evaluated with the help of light microscopy with hematoxylin and eosin and Van Gieson staining: fibrinoid necrosis, metachromasy, karyorhexis and karyolisis, fibrinoid swelling and myxomatosis. Objectification of the abovementioned changes was achieved by morphometrical investigations; semi-numerical indexes of pathological processes and quantitative values of fibrinoid necrosis spreading, which were evidently higher in the materials of the first group and had the transmural character of the damage.

The observed mean comparative optic density of PA wall and disintegration specific area of the connective tissue were evidently lower in the first experimental group in relation to the second group of the investigation ($p < 0.001$), the minimum mean optic density was obtained in the samples of the tissues of subgroup 1B.

Especially evident changes were observed in "the edge zones" (subgroup 1B), they occurred in the form of increased spreading depth of fibrinoid necrosis and metachromasy spreading onto medial and intimal layers, and also occurred in the form of the decreased optic density of the investigated tissues in relation to similar samples from the central zones.

In the second experimental group the tendency to greater alteration in subgroup 2B in relation to subgroup 2A was preserved. However, in subgroup 2B the abovementioned changes were not evidently determined in the intimal layer and did not have transmural character. The endothelium damage observed in the preparations of subgroup 2B, apparently had the mechanical genesis due to the formation of arterial wall duplication under the ablator clamp jaws.

ICH analysis of the preparations allowed qualitatively evaluating the damage of trunks and endings of peripheral nerve fibers in adventitial and intimal layers of PA cut after radiofrequency exposure in the experimental groups.

In the first experimental group the active expression of synaptophysin and protein S-100 of sympathetic nerve fibers was absent in adventitial and, as a rule, intimal layers. In the

preparations obtained from PAs of the animals of the second experimental group, synaptophysin activity in synaptic fibers and expression of S-100 protein of vasa vasorum endothelium were also not determined in the adventitial layer, at the same time, the positive reaction of protein S-100 and synaptophysin was revealed in nerve endings and ganglia in PA intimal layer of the preparations of the second group.

Thus, in the experiment on animals when conducting PA circular denervation, the application of subthreshold rates of radiofrequency exposure corresponding to 50% value of the impedance of PA tissues from the corresponding impedance values under transmural damage allowed avoiding irreversible damages of nerve endings and ganglia of PA intimal layer, thus preserving the physiological neuroreflectory regulation of PA and the whole pulmonary circulation. The results obtained during the experiment demonstrate the efficiency of radiofrequency ablation of sympathetic ganglia and nerve fibers of the adventitial layer along the entire circumference of PA cut when reaching 50% level of the tissue impedance in relation to the impedance level at the moment of transmural damage. Thus, the cascade of pathological reflexes, factors of LH advance connected with the spasm of precapillary mouth of pulmonary arterioles is turned off.

## References


1. Iung B. A prospective survey of patients with valvular heart disease in Europe: The Euro Heart Survey on Valvular Heart Disease. European Heart Journal 2003;24:1231-43. DOI: 10.1016/s0195-668x(03)00201-x.
2. Goldbarg S.H., Elmariah S., Miller M.A., Fuster V. Insights into degenerative aortic valve disease. J Am CollCardiol 2007;50:1205-13. DOI: 10.1016/j.jacc.2007.06.024.
3. Fedorov S.A., Medvedev A.P., Chiginev V.A., Zhurko S.A., Gamzaev A.B., Tselousova L.M. Comparative assessment of clinical and hemodynamic results of implantation of xenoaortal and xenopericardial biological prostheses during the correction of degenerative defects of aortal valve // Complex problems of cardiovascular diseases. – 2018. – V. 7, № 2. – P. 50-60. UDK: 616.127-007-089.844-77. ISSN: 2306-1278. eISSN: 2587-9537.
4. Trofimov N.A., Medvedev A.P., Dragunov A.G., Babokin V.E., Nikol'skiy A.V., Mizurova T.N. et al. Denervation of pulmonary trunk and pulmonary orifice in patients with surgically corrected mitral valve disease against high pulmonary hypertension. Almanac of Clinical Medicine 2017;45:192-99. DOI:10.18786/2072-0505-2017-45-3-192-199.
5. Trofimov N.A., Medvedev A.P., Babokin V.E. et al. The effectiveness of surgical treatment of mitral regurgitation, with atrial fibrillation of non-ischemic etiology. Medical almanac 2014;5(35):165 169.
6. Medvedev A.P., Skopin I.I., Chiginev V.A., Trofimov N.A., Fedorov S.A., Zhiltsov D.D., Zemskova E.N. Key aspects of of heart valve surgery development // Medical almanac. – 2015. – №3. – P. 32-38. UDK: 616.127-089-03. ISSN: 1997-7689eISSN: 2499-9954
7. Zhurko S.A., Fedorov S.A., Chiginev V.A., Medvedev A.P., Pichugin V.V., Lashmanov D.I., Shirokova O.R., Zhiltsov D.D., Tselousova L.M. Modern approach to surgical treatment of infectious endocarditis // Medical almanac. – 2017. – №3. – P. 95-98. https://doi.org/10.21145/2499-9954-2017-3-95-98 UDK: 616.126.3-002-089:616.9 ISSN: 1997-7689 eISSN: 2499-9954
8. Bockeria L.A., Shengelia L.D. Treatment of atrial fibrillation. Part II. Current realities and future prospects. Annalyaritmologii 2014;11:76-86.
9. Babokin V.E., Trofimov N.A. Prevention of Atrial Fibrillation Recurrence after the Maze IV Procedure. Ann ThoracSurg 2019. DOI: 10.1016/j.athoracsur.2019.08.087
10. Sulimov V.A., Lishuta A.S. Prospects for the Treatment of Patients with Atrial Fibrillation. Rational Pharmacotherapy in Cardiology 2011;7:323-33.
11. Trofimov N.A., Medvedev A.P., Babokin V.E., Demarin O.I., Zhamlikhanov N.K., Dragunov A.G. et al. Surgical Treatment of Complex Arrhythmias in Patients with Non-Ischemic Mitral Insufficiency. Almanac of Clinical Medicine 2016:64-73.
12. Zheleznev S.I., Demidov D.P., Afanasiev A.V., Nazarov V.M., Demin I.I., Bogachev-Prokofiev A.V. et al. Radiofrequency Denervation of Pulmonary Artery in Surgery of Dysplastic Mitral Valve Defects with Severe Pulmonary Hypertension. Russian Journal of Cardiology 2016:70-72.
13. Galie N., Humbert M., Vachiery J.L., Gibbs S., Lang I., Torbicki A. et al. 2015 ESC/ERS Guidelines for the diagnosis and treatment of pulmonary hypertension. Eur Heart J 2016;37:67-119. DOI: 10.1093/eurheartj/ehv317
14. Porodenko N.V., Skibitskiy V.V., Zapevina V.V. The diagnosis and treatment of primary pulmonary hypertension: a modern view on the problem. Kuban Scientific Medical Bulletin.2014;(3):140-144. (In Russ.) https://doi.org/10.25207/1608-6228-2014-3-140-144.
15. Rubin L.J. Primary pulmonary hypertension. N Engl J Med 1997;336:111-7. DOI: 10.1056/NEJM199701093360207.
16. Gaine S. Pulmonary hypertension. JAMA 2000;284:3160-8. DOI: 10.1001/jama.284.24.3160
17. Simonneau G., Gatzoulis M.A., Adatia I, Celermajer D, Denton C, Ghofrani A et al. Updated clinical classification of pulmonary hypertension. J Am CollCardiol 2013;62:D34-41. DOI: 10.1016/j.jacc.2013.10.029
18. Trofimov N.A., Medvedev A.P., Babokin V.E., Dragunov A.G., Efimova I.P., Gartfelder M.V. et al. Effectiveness of PADN-procedure in patients with high pulmonary hypertension against background of mitral valve dysfunction complicated by atrial fibrillation and effect on preservation of sinus rhythm in postoperative period. Medical alphabet Cardiology 2018;4:18-24.
19. Briongos Figuero S., Moya Mur J.L., Garcia-Lledo A., Centella T., Salido L., Acena Navarro A. et al. Predictors of persistent pulmonary hypertension after mitral valve replacement. Heart Vessels 2016;31:1091-9. DOI: 10.1007/s00380-015-0700-2
20. Osorio J., Russek M. Reflex changes on the pulmonary and systemic pressures elicited by stimulation of baroreceptors in the pulmonary artery. Circ Res 1962;10:664-7. DOI: 10.1161/01.res.10.4.664.
21. Baylen B.G., Emmanouilides G.C., Juratsch C.E., Yoshida Y., French W.J., Criley J.M. Main pulmonary artery distention: A potential mechanism for acute pulmonary hypertension in the human newborn infant. The Journal of Pediatrics 1980;96:540-44. DOI: 10.1016/s0022-3476(80)80863-8.
22. Juratsch C.E., Jengo J.A., Castagna J., Laks M.M. Experimental pulmonary hypertension produced by surgical and chemical denervation of the pulmonary vasculature. Chest 1980;77:525-30. DOI: 10.1378/chest.77.4.525.
23. Guazzi M., Vitelli A., Labate V., Arena R. Treatment for pulmonary hypertension of left heart disease. Curr Treat Options Cardiovasc Med 2012;14:319-27. DOI: 10.1007/s11936-012-0185-6.
24. Chen S.L., Zhang F.F., Xu J., Xie D.J., Zhou L., Nguyen T. et al. Pulmonary artery denervation to treat pulmonary arterial hypertension: the single-center, prospective, first-in-man PADN-1 study (first-in-man pulmonary artery denervation for treatment of pulmonary artery hypertension). J Am CollCardiol 2013;62:1092-100. DOI: 10.1016/j.jacc.2013.05.075.
25. Bogachev-Prokofiev A.V., Zheleznev S.I., Afanasyev A.V., Fomenko M.S., Demidov D.P., Sharifulin R.M. et al. Denervation of pulmonary artery during mitral valve surgery in patients with high pulmonary hypertension // Pathology of blood circulation and cardiosurgery;19:19-25. DOI: 10.21688/1681-3472-2015-4-19-25.
26. Trofimov N.A., Medvedev A.P., Dragunov A.G., Nikolskiy A.V., Mizurova T.N., Gartfelder M.V. et al. Method of surgical treatment of secondary pulmonary hypertension in the case of patients having

surgical correction of mitral valve pathology. Medical almanac 2017:33-37. DOI: 10.21145/2499-9954-2017-3-33-37.
27. Trofimov N.A., Medvedev A.P., Babokin V.E., Efimova I.P., Kichigin V.A., Nikolsky A.V. et al. Changing the quality of life after the PADN procedure in patients with mitral valve dysfunction, complicated by atrial fibrillation and severe pulmonary hypertension. Bashkortostan medical digest 2019;14;2(80):8-17.
28. Lillie R.D. Histopathologic technic and practical histochemistry. Moscow: Mir Publ., 1969.
29. Glantz S.A. Primer of Biostatistics. Moscow: Praktika Publ, 1998.